Direct observation of the directional walk of single adatoms and the adatom polarizability*

T. T. Tsong and Gary Kellogg
Department of Physics, The Pennsylvania State University, University Park, Pennsylvania 16802
(Received 19 August 1974; revised manuscript received 20 January 1975)

Using the field-ion microscope, it is possible to observe the directional walk of an adatom on an atomically perfect metal surface. The driving force arises from the polarization binding in a nonuniform electric field on a crystal plane. From the average velocity of the walk the polarizability of the adatom can be calculated. A systematic study of single 5-*d* transition-metal atoms adsorbed on the (110) plane of W was made and the adatom polarizabilities obtained. These values were found to be significantly less than the free-atom polarizabilities. It will be shown that the polarizability of chemisorbed atoms arises mainly from a field-induced charge transfer between the adatom and the substrate plane, and is thus very closely related to the electronic density of states of the adatom. For a W adatom adsorbed on the W (110) plane the average density of states in the range from -5.3 to -7.2 eV is estimated to be ~ 0.75 eV^{-1} per adatom.

I. INTRODUCTION

The possibility of using the field-ion microscope (FIM) to investigate the surface diffusion of adatoms thermally deposited from a side arm coil source was shown by Müller[1] just one year after the FIM had achieved its full atomic resolution. Since then, a number of quantitative investigations of the random-walk diffusion of various single atoms on perfect crystal planes of various metals have been reported.[2-5] In the random-walk diffusion, the surface potential as seen by an adatom is symmetric; thus the adatom does not experience a driving force. When a driving force is present, the surface potential is no longer symmetric, and the walk of the adatom becomes directional. The directional walk of an adatom on a W (110) plane, due to the attraction of either an impurity atom or a lattice defect in the substrate plane, was reported earlier.[4] The directional walk of single tungsten adatoms by a controllable driving force, arising from the polarization binding of the adatom in an applied nonuniform electric field, was investigated by Tsong and Walko[6] under modest vacuum conditions. The FIM used was not equipped with an accurate temperature control of the emitter. Here we report an investigation of the directional walk of single 5-*d* transition-metal adatoms on the atomically perfect tungsten (110) plane under an applied nonuniform electric field. We derive the adatom polarizability from the average velocity of the directional walk and point out how this quantity differs from the free-atom polarizability and how it is related to the electronic density of states of the adatoms.

II. DIRECTIONAL WALK

A. General principles

An adatom on a perfect crystal plane performs discrete random walks at a relatively low temperature. In the absence of a driving force, the surface potential barrier as seen by the adatom is symmetric. The walk is in random directions. A discussion of the symmetric random-walk (henceforth it will be abbreviated as random-walk) diffusion of adatoms appropriate for FIM investigations has been given by Ehrlich.[7] Here we discuss briefly the asymmetric discrete random walk (or the directional walk) of an adatom in an unbounded one-dimensional lattice due to a driving force.

From the theory of random walks, it is well known that

$$\langle \rho \rangle = Nl(p-q) \tag{1}$$

$$\langle \rho^2 \rangle = Nl^2 + [(N-1)/N]\langle \rho \rangle^2 , \tag{2}$$

where ρ denotes the spatial coordinate, N is the total number of jumps, l is the jumping distance, and p and q are, respectively, the probability of jumping toward the right and toward the left. For the symmetric random walk, $p = q = \frac{1}{2}$,

$$\langle \rho \rangle = 0, \quad \text{and} \quad \langle \rho^2 \rangle = Nl^2 . \tag{3}$$

When a driving force is present, the potential barrier becomes asymmetric.[8] The barrier heights toward right and toward left will be represented, respectively, by E_R and E_L. As we are concerned mainly with the diffusion of heavy-metal atoms, the tunneling effect is negligibly small and will be omitted. The directional walk is achieved by thermal activations. Thus,

$$\langle \rho \rangle = \nu_0 \tau l (e^{-E_R/kT} - e^{-E_L/kT}), \tag{4}$$

where τ is the time interval of observation and ν_0 is the atomic vibrational frequency given approximately by kT/h. Equation (4) takes a simple form if the potential energy gradient β_E is constant and the surface potential has sharp maxima at middle points of two neighboring adsorption sites. One then obtains[9]

$$\langle \rho \rangle = 2\nu_0 \tau l\, e^{-E_d/kT} \sinh(\beta_E l/2kT). \quad (5)$$

where E_d is the activation energy of surface diffusion in the absence of the driving force.

B. Driving force by a nonuniform electric field

Surface diffusion under an applied electric field has been investigated by Bettler and Charbonnier,[10] Utsugi and Gomer,[11] and Swanson *et al.*[12] using field-emission microscopy, and by Graham and Ehrlich[13] using field-ion microscopy. All of them assume the electric field to be uniform; thus their data analysis is based on the symmetric random-walk diffusion. The first observation, as well as analysis of single-atom diffusion with a controllable driving force produced by a nonuniform electric field, was reported by Tsong and Walko.[6] We shall consider here the many possible effects of an applied field on the diffusion of an adatom on a perfect one-dimensional crystal surface. Let us assume first that the electric field is uniform. It is well known that the dipole moment p of an adatom in an electric field can be expressed as[14,15]

$$p = \mu + \alpha E + \tfrac{1}{6}\gamma F^3 + \cdots, \quad (6)$$

where μ is the surface-induced dipole moment and α and γ are the polarizability and the hyperpolarizability of the adatom. It should be recognized that α and γ for an adatom are necessarily different from those for a free atom, as will be discussed later. The energy of the adatom on the plane is reduced by an amount

$$\Delta E = -\mu F - \tfrac{1}{2}\alpha F^2 - \tfrac{1}{24}\gamma F^4 - \cdots \quad (7)$$

by the applied field. Utsugi and Gomer[11] point out that the dipole moment and the polarizability of an adatom at the saddle and the trough positions of the surface potential may be different. The electric field at the saddle and trough position may also be different. As a result, the activation energy of surface diffusion in the applied uniform electric field is given by

$$E_d(F) = E_d(0) - (\mu_s F_s - \mu_t F_t) - \tfrac{1}{2}(\alpha_s F_s^2 - \alpha_t F_t^2) - \tfrac{1}{24}(\gamma_s F_s^4 - \gamma_t F_t^4) - \cdots, \quad (8)$$

where the subscripts s and t refer to the saddle and trough positions of the surface potential. By neglecting the second-order terms and the hyperpolarizability contribution, Eq. (8) can be rewritten as

$$\Delta E_d = E_d(0) - E_d(F) \approx \mu_t \Delta F + F_t \Delta\mu + \alpha_t F_t \Delta F + \tfrac{1}{2}(\Delta\alpha) F_t^2, \quad (9)$$

where

$$\Delta\mu \equiv \mu_s - \mu_t, \quad \Delta\alpha \equiv \alpha_s - \alpha_t, \quad \Delta F \equiv F_s - F_t. \quad (10)$$

It is obvious that by measuring the reduction in the activation energy of surface diffusion by the applied field, $\Delta\mu$ and $\Delta\alpha$ can be derived. It should be realized that these are not the dipole moment and the polarizability of the adatom. Based on this principle, Swanson *et al.*[12] obtain a $\Delta\alpha$ of about 60 Å^3 for cesium adatoms on the tungsten surface, which is comparable to the free cesium atom polarizability. This large value of $\Delta\alpha$ is due to the omission of the effect of the driving force. It is clear from Eq. (2), by treating the directional-walk problem as a random walk, one grossly overestimates the mean-square displacement and ΔE_d and, therefore, $\Delta\mu$ and $\Delta\alpha$ also. As will be shown in Sec. IV, our result gives the adatom polarizabilities to be much less than the free-atom polarizabilities and also provides convincing evidence of the occurrence of a chemical specific charge-transfer effect.

It is a well-known fact that the electric field on FIM emitter surface varies from one plane to the other. Even on a flat plane, the electric field varies from location to location.[15,16] For example, the electric field at the center of the largest obtainable W (110) plane on a FIM emitter, prepared by a field evaporation at 10^{-1}–10^{-2} layer/sec, is about 14% lower than that at the edge of the plane.[15] This is schematically shown in Fig. 1(a). The field

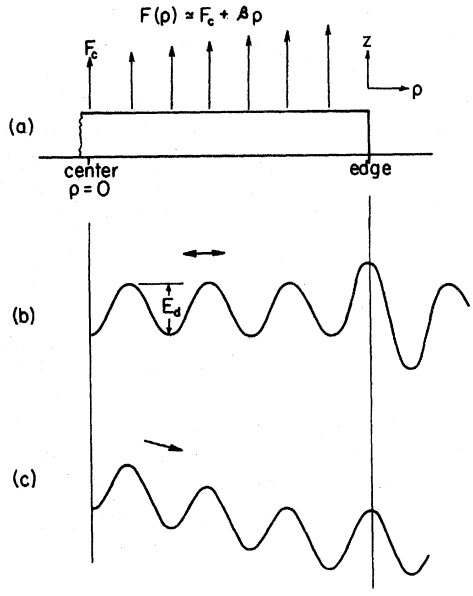

FIG. 1. (a) Schematic diagram showing the electric field distribution on a flat plane in an applied voltage. (b) Surface potential barrier as seen by an adatom in the absence of an applied field is symmetric. The migration of the adatom is in a random direction. (c) In an applied field the surface potential is inclined by a polarization binding. The migration of an adatom becomes directional.

gradient is very much a constant except very close to the center and the edge of the plane. Our discussion of the driving force effect is confined to the constant-field-gradient case.

The detailed form of the periodic surface potential is not known. We will represent it by the first Fourier component,

$$U(\rho, 0) = \tfrac{1}{2} E_d [1 - \cos(2\pi\rho/l)]. \quad (11)$$

In an applied field, the polarization energy has to be included. Thus,

$$U(\rho, F) = U(\rho, 0) - \mu(\rho) F(\rho) - \tfrac{1}{2} \alpha(\rho) F^2(\rho), \quad (12)$$

where

$$F_s(\rho) = F_{cs} + \beta\rho,$$
$$F_t(\rho) = F_{ct} + \beta\rho. \quad (13)$$

Here, F_c is the field at the center of the plane and β is the field gradient. By finding E_R and E_L for the potential and substituting them into Eq. (4), one gets

$$\langle \rho \rangle_F \approx 2\tau l \nu_0 e^{-E_d/kT} \times \exp\left[\left(\Delta E_d - \frac{(\alpha_t + \mu_t/F_{ct})^2 \beta^2 F_{ct}^2 l^2}{2\pi^2 E_d^2}\right)\Big/ kT\right] \times \sinh[(\alpha_t + \mu_t/F_{ct})\beta F_{ct} l/2kT]. \quad (14)$$

If we confine our attention to closely packed smooth planes, such as the (110) of a bcc and the (111) of a fcc, where $\Delta F \approx \Delta\mu \approx \Delta\alpha \approx 0$, as will be discussed in Sec. IV B, one finds

$$\langle \rho \rangle_F = 2\tau l \nu_0 e^{-E_d/kT} \sinh[(\mu\beta l + \alpha\beta F_c l)/2kT]. \quad (15)$$

But

$$\langle \rho^2 \rangle_0 = Nl^2 = \tau l^2 \nu_0 e^{-E_d/kT}. \quad (16)$$

Therefore

$$\langle \dot{\rho} \rangle_F = (2\langle \rho^2 \rangle_0 / l\tau) \sinh[(\mu\beta l + \alpha\beta F_c l)/2kT], \quad (17)$$

or

$$\mu + \alpha F_c = (2kT/\beta l) \sinh^{-1}(l\langle \dot{\rho} \rangle_F \tau / 2\langle \rho^2 \rangle_0). \quad (18)$$

In other words, we have expressed μ and α in terms of experimentally measurable quantities β, F_c, T, τ, $\langle \dot{\rho} \rangle_F$, and $\langle \rho^2 \rangle_0$.

C. The effect of the image gas

As will be described in Sec. III, both the random-walk and the directional-walk experiments were performed under an image-inert-gas pressure of 10^{-4} Torr. It is important to estimate here the effect of the image gas. There are three effects which must be considered, namely, the field adsorption of the image-gas atoms,[17] the bombardment of the gas atoms, and the electron shower from the imaging process.[18]

In the operational condition of the FIM, all of the imaged surface atoms are field adsorbed with an image-gas atom. The field adsorption, however, disappears above 150 K for both He and Ne.[17] Our directional-walk experiments were all carried out above 200 K, thus no field adsorption was expected. For the random-walk experiment, no field was applied; therefore, there was no field adsorption in this case either.

The effect of gas bombardment on the random walk of an adatom can be estimated as follows. The kinetic gas flux per unit area per unit time to a surface is given by

$$Z = p/\sqrt{2\pi M_g kT}, \quad (19)$$

where M_g is the mass of the gas atom and p is the gas pressure. For each gas-atom impact, an energy of about $2akT$ is transfered to the adatom, where a is the thermal accommodation coefficient. Assuming that the adatom stays at the higher energy state for n atomic vibrations, then the number of gas-impact-assisted atomic jumps per unit time is given by

$$\Delta N \approx nZ\pi(r_s + r_g)^2 \exp[-(E_d - 2akT)/kT], \quad (20)$$

where r_s and r_g represent, respectively, the radius of the surface atom and the gas atom. The number of atomic jumps per unit time in vacuum is given by

$$N = \nu_0 e^{-E_d/kT} \approx (kT/h) e^{-E_d/kT}. \quad (21)$$

Thus their ratio is given by

$$\Delta N/N \simeq [nZ\pi(r_s + r_g)^2 h/kT] e^{2a}. \quad (22)$$

For helium as the image gas, $r_s + r_g \approx 2.6$ Å, and $a \approx 0.05$ or less.[19] The value of n is more difficult to estimate. A computer investigation of the dynamics of the bulk diffusion of an impurity atom in a lattice of 256 atoms shows that any excess energy in the impurity atom is dissipated to the lattice in a few atomic vibrations.[20] Since we are making an order-of-magnitude estimate here, $n \approx 10$ will be assumed. At 300 °K and $p = 10^{-4}$ Torr, $\Delta N/N \approx 7.7 \times 10^{-9}$ is obtained. It is clear that the gas impacts will produce no detectable effect.

In the directional-walk experiment, the applied field not only increases the gas flux, it also increases the impact energy. An incoming gas atom, upon its first impact to a surface atom in an applied field F, will transfer an energy of $a[\frac{1}{2} f\alpha F^2 + 2kT]$ to the surface atom, where $f \approx 6$ is the enhancement factor due to a field-induced dipole-dipole interaction between the surface atom and the gas atom.[17] An accurate estimate of the gas flux is much more difficult in this case. But experimentally it is known that about 10^4 image-gas ions originate from a bright surface atom at 78 °K cooling and a 10^{-4}-Torr gas pressure.[21] This number should be nearly equal to the primary gas flux at that temperature.

At 300 °K, the number is reduced to $10^4 \times \frac{78}{300} = 2.6 \times 10^3$ sec^{-1}. Secondary impacts due to the hopping motion of the image-gas atoms, while much larger in number, have a much smaller energy transfer. The effect of the secondary impacts should be about the same order of magnitude as the primary impacts. Now

$$\frac{\Delta N}{N} \approx \frac{2.6\times 10^3 hn}{kT} \exp[a(\tfrac{1}{2}\alpha f F^2 + 2kT)/kT] \approx 1.64\times 10^{-8}. \quad (23)$$

Again we conclude that the gas impacts will produce no observable effect on the directional walk. We can also roughly estimate the primary gas flux using the supply function given by Southon.[21]

$$Z' = \pi(r_s + r_g)^2 [p/(2\pi M_g kT)^{1/2}](\pi\phi)^{1/2}, \quad (24)$$

with

$$\phi = f\alpha F^2/2kT. \quad (25)$$

At 10^{-4} Torr, Eq. (24) gives a flux of 2×10^3 sec^{-1}, comparable to that estimated from the field ion current. Equation (24) is valid really for dipoles in a Coulomb field. For the dipole-dipole attraction, the range of the force is much shorter. By using the equation above, we can only overestimate the gas supply. Since $\Delta N/N$ is so small, whatever the inaccuracy in our estimation of the primary gas flux may be, it is unlikely to affect our conclusion.

It is important to realize that ΔN is directly proportional to the gas pressure. The incoming gas atoms, with their momentum nearly parallel to the radial direction of the tip, have momentum components pointing toward the plane center. They could only reduce the velocity of the directional walk if such a small effect could indeed be detected.

Another effect we have to consider is the electron shower from the field-ionization process.[18] With a 10^{-4}-Torr gas pressure at 226 °K or above, and a field well below or at the best image field of the image gas, no field-ion image can be seen, even with a channel plate image intensification. The electron-shower effect will be negligible with such a small ion current density during the directional-walk experiment, especially since field ionization occurs in a very narrow zone (~0.3 Å) at or below the best image field.

III. EXPERIMENTAL TECHNIQUES

The general principles of operation and design of the FIM can be found elsewhere.[21] We describe here only some of the special features of the bakable UHV stainless steel FIM used in this experiment. As shown in Fig. 2, a cylindrical sapphire piece with four 0.03-in. holes perpendicular to the cylindrical axis is used for supporting the emitter mounting loop. The sapphire piece is tightly attached to a copper plate by two screws. The copper plate is silver soldered to the bottom of the stainless steel cold finger. The tungsten field-ion emitter is spot welded on a 0.004-in. platinum loop with two 0.001-in. spot-welded platinum potential leads. Both the loop and the potential leads are tightly plugged into the 0.03-in. holes with tungsten plugs. With this design, very satisfactory cooling of the specimen is achieved, and no high-voltage breakdown has ever occurred.

The FIM is equipped with a microchannel plate for image intensification. For the directional-walk experiment, we have to apply an electric field of 2–4.5 V/Å to the emitter surface, and simultaneously heat the tip to a temperature where random-walk diffusion just starts, which is about 220–300 °K. Accurate control and monitoring of the emitter temperature is difficult for the ordinary design of the FIM where the imaging voltage is applied to the emitter side. In this experiment, the imaging voltage, as well as the voltage needed to produce a directional walk, is applied to a stainless steel conical-shaped electrode placed at the screen side. The tip assembly is kept at or near ground potential at all times.

As in other sensitive-surface experiments, the cleanliness of the surface is essential in obtaining meaningful experimental results. Our system is equipped with an oil diffusion pump, a Vac-Ion pump, and a titanium sublimation pump. After an extensive initial vacuum processing, an overnight baking at 250 °C and a careful degassing routinely give vacuums in the 10^{-11}-Torr range. The over-

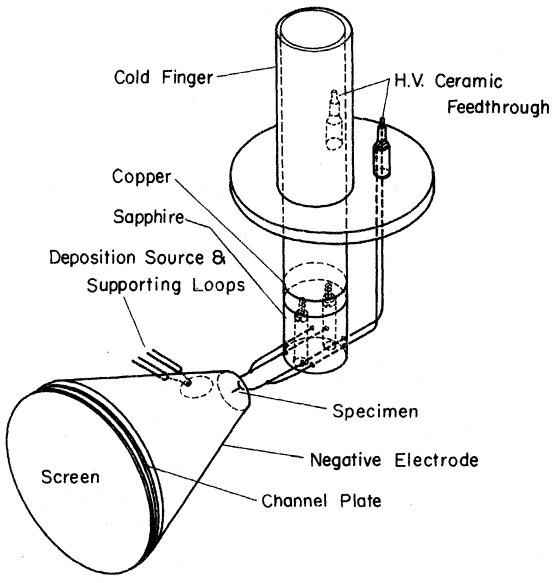

FIG. 2. Schematic diagram showing the essential parts of the field-ion microscope used in this experiment.

night baking was repeated about once a week, even without an opening of the system. We find no contamination problem with the microchannel plate if it is operated under modest gain. It is most essential that all degassings, including the deposition source coils and their supporting loops made of 0.05-in. nickel, are done while the system is hot. Before the system is valved off from the diffusion pump and the Vac-Ion pump, the titanium getter is activated and cooled down to liquid-nitrogen temperature. Helium gas of 2×10^{-4} Torr is admitted to the system by diffusion through a Vycor-glass bulb at 350 °C. The helium is supplied from a spectroscopy grade helium bottle. With this double precaution, the purity of the helium in the system is ensured. The experiment with Ta adatoms was carried out with neon as image gas. In this case, the spectroscopy grade neon was first admitted to a liquid-nitrogen-cooled active titanium getter bulb, where it stayed for at least 30 min before being admitted to the system. With these procedures, we generally find no problem with contaminations. No change of even a single atom is detected on an emitter surface when turning the imaging voltage off for 5 min. In a few cases where contamination occurred, which could be detected from a loss of adatoms or substrate atoms at slightly lower fields than their expected desorption fields, the sets of data were discarded and the system was rebaked. The tip temperature is controlled by resistive heating of the 0.004-in. Pt tip mounting loop with an electronically regulated constant voltage dc power supply, which monitors directly the potential difference at the potential leads. With this simple procedure, the tip temperature reaches its preset value in less than 7 sec without any overshoot. The temperature is reproducible to about 0.2 °K. For the random-walk diffusion experiments with heating periods of 1–3 min each, the slow rise time causes an error smaller than $\frac{1}{2}\%$ in the measured value of $\langle\rho^2\rangle$, which is small compared to the statistical fluctuations of the experiment.[5] A temperature calibration is done on the system after each baking. For the directional-walk experiment, the emitter is set at a temperature where the random-walk diffusion starts to be detectable. After the heating current is turned on for 10 sec, allowing the tip temperature to stabilize, a high dc voltage is applied for 10–30 sec. The tip is then cooled down for image recording. During the 10-sec preheating period in zero field, no movement of the adatom is expected. The high voltage is supplied from a well-regulated dc power supply which reaches its preset value in less than 0.5 sec. The voltage is adjusted to produce a drifting velocity of about 0.2 Å/sec; thus, an adatom near the center of a plane moves over to the plane edge in three to four periods.

The field calibration is based on the recent work of Sakurai and Müller.[22] Using the energy distribution of field ionization, they were able to obtain the field strength above the center of a plane with a 3% accuracy. According to these authors, the electric field at the center of a W (110) plane field evaporating at a rate of ~0.1 layer/sec at 78 °K cooling is 5.70 V/Å.

All of the micrographs were taken with liquid-nitrogen cooling of the specimen. The adatom displacements were determined by either the color-superposition technique or by means of internal fiduciary marks, i.e., lattice atoms. Magnification of the micrographs was calibrated with the spacings of the (211) atomic rows. All data reported here were taken from a single adatom on a perfect W (110) plane prepared by field evaporation of the emitter surface. The W (110) planes were the maximum sizes obtainable at a field evaporation rate of about 10^{-1} layer/sec. For the directional-walk experiment, the adatom always started at a position about $\frac{1}{3}R$ away from the plane center, where R is the average radius of the plane. Once the adatom reached the plane edge, it was brought back near to the center of the plane with great patience by random-walk diffusion, which then provided data for the needed mean-square displacement in zero field. To avoid excess boundary effects, however, only data taken of the adatom away from the plane edge were accepted. The mean-square displacement in zero field and the drifting velocity in the applied field were measured under the same emitter temperature calibration. Typically, 15–20 complete directional walks (from near the plane center to the plane edge) were measured for one metal. For the random-walk data, about 40 heating periods were performed for a metal at one temperature. Figure 3 shows the directional walk of an Ir adatom on a W (110) plane.

The directional walk of W, Re, Ir, and Pt can be observed continuously by using $\sim5\times10^{-3}$ Torr helium and by operating the channel plate at high gains.[6] The contrast of the adatom is greatly enhanced if Ne-Ar mixed gas is used for imaging. Figure 4 shows an example of the directional walk of a W adatom with the FIM operated at room temperature. Although the directional walk of the adatom can be most vividly seen, we did not use this procedure for obtaining quantitative data for the following reasons:

(a) The good vacuum cannot be maintained with the channel plate operated at high gains because of the degassing problem.

(b) If pure helium is used for imaging, image contrast is so low that an adatom near the center of a plane is hardly visible. If, on the other hand, a Ne-Ar mixture is used, the field adsorption of

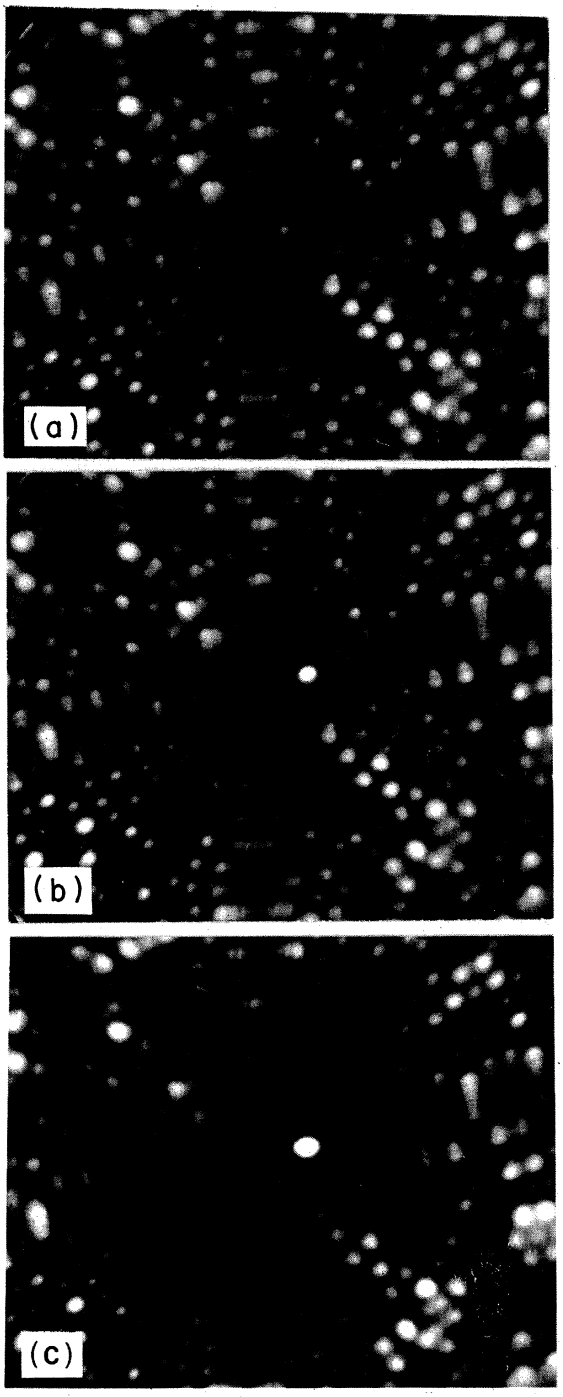

FIG. 3. Helium FI micrographs showing the directional walk of an Ir adatom on a W (110) plane. Between two sucessive adatom locations, the emitter was maintained at 296 °K with an applied field of 3.9 V/Å for 15 sec. The micrographs were taken at 4.5 V/Å and 78 °K.

Ar may affect the accuracy of the data.

(c) The electron shower effect may be a problem with a Ne-Ar mixture for the Re, Ir, and Pt adatom experiments. To avoid this uncertainty all the quantitative data reported here were obtained with the precedures described earlier.

IV. EXPERIMENTAL RESULTS AND DISCUSSIONS

A. Random walk on the W (110) plane

The random-walk diffusion of single adatoms on a perfect crystal plane is a subject of considerable interest in itself[2-5]; however, its use in this investigation is limited to providing the mean-square displacement data needed in deriving the polarizability of adatoms. An important consideration in random-walk diffusion experiments is the uncertainty of the temperature calibration. For most investigations, the accuracy in the calibration of temperature increments is 0.5 °K or better; but the absolute temperature calibrations of different investigators may differ by as much as 5 °K, simply from the fact that the temperature is not uniform along the tip mounting loop. This will give an uncertainty in $\langle \rho^2 \rangle_0$ of 100%, which is intolerable for our purpose. We have confined our measurements of $\langle \rho^2 \rangle_0$ of all the adatoms to the same temperatures where the directional-walk measurements were carried out. The data obtained are listed in Table I. We did, however, obtain the temperature dependence of $\langle \rho^2 \rangle_0$ for an Ir adatom on a W (110) plane, which is shown in Fig. 5. From this plot, an activation energy $E_d = 0.70$ eV and a diffusivity $D_0 = 1 \times 10^{-5}$ cm^2/sec are obtained. A similar result with a few adatoms on a W (110) plane was reported earlier.[3] For single-atom diffusion on the W (110) plane, D_0 has been found to

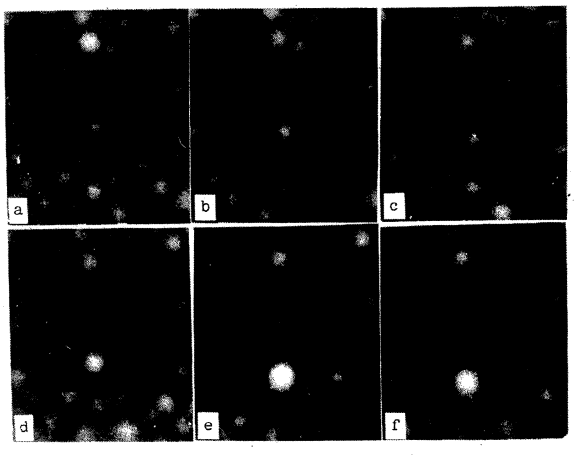

FIG. 4. Continuous observation of the directional walk of a W adatom on a W (110) plane at ~3.8 V/Å and ~295 °K. A Ne-Ar mixed gas of $\sim 6 \times 10^{-3}$ Torr was used for the imaging. The good contrast of the image at such a high temperature results from the field adsorption of Ar atoms. Although the directional walk of the adatom was most vividly seen with this technique, it was not used to derive the quantitative data. The reasons are discussed in the text.

TABLE I. Experimental results of the directional walk.

	Ta	W	Re	Ir	Pt
T(°K)	238	302	310	296	226
$\frac{\langle\rho^2\rangle_0}{\tau}$ (Å²/sec)	0.27	0.20	0.083	0.33	0.27
F_c (V/Å)	1.87	2.35	3.50	3.90	4.50
$\langle\dot{\rho}\rangle_F$ (Å/sec)	0.29	0.13	0.076	0.24	0.27
β (V/Å²)	0.012	0.0155	0.0245	0.019	0.020
α (Å³)	12.74±0.16	7.0±0.8	4.09±0.59	3.28±0.38	2.74±0.33
Electronic configuration	$5d^36s^2$	$5d^46s^2$	$5d^56s^2$	$5d^76s^2$	$5d^96s^1$
α_a (Å³)[a]	19.4	16.8	15.0	12.5	11.5

[a]From Ref. 25.

be consistently in the 10^{-3}–10^{-5}-cm²/sec range.[2,3] By taking a $D_0 = 10^{-3}$ cm²/sec, the activation energy of all the other adatoms can be derived from

$$D = \langle\rho^2\rangle_0/4\tau = D_0 e^{-E_d/kT}, \tag{26}$$

with an uncertainty in E_d of ~± 0.05 eV. The result is shown in Fig. 6. Such d-electron dependence of E_d has been found earlier by Bassett and Parsley.[3]

B. Directional walk on the W (110) plane

The directional walk of adatoms follows the direction of the maximum field gradient, when there is no other constraint, which is in the radial direction of the plane. It is very much one dimensional, even on a two-dimensional plane. The equations derived for a one-dimensional lattice may still be used with a slight modification. There is some evidence that the migration of an adatom even on a smooth plane is along the surface channels.[9] The channel acts as a constraint for the directional as well as the random walks. The W (110) surface channel is nearly hexagonal in structure. This hexagonal constraint causes the individual atomic jumps in the directional walk to be in the direction of $\frac{1}{2}\sqrt{3}$ maximum field gradient. Thus, Eq. (18) is modified to be

$$\mu + \alpha F_c = \frac{2kT}{0.867\beta l} \sinh^{-1}\left(\frac{l\langle\dot{\rho}\rangle_F \tau}{2\langle\rho^2\rangle_0}\right). \tag{27}$$

While the individual steps are slightly off the radial direction, the path is still very much in the radial directions of the plane, as shown both in Figs. 3 and 4.

In principle, one can obtain values of both μ and α from the intercept and the slope of a $(2kT/0.867\beta l)\sinh^{-1}(l\langle\dot{\rho}\rangle_F\tau/2\langle\rho^2\rangle_0)$ vs F_c plot. In practice, due to the small size of the W (110) planes obtainable with the FIM, the experiment can only be conveniently carried out in a very narrow field range, typically in 0.5 V/Å range out of a total of ~3 V/Å. Furthermore, the statistical fluctuations in single-atom experiments are considerable. It is therefore inpractical to obtain such a plot. Fortunately, the dipole moment of single metallic adatoms has been found[23,24] to be about 0.3–0.7 debeye (1 D ≡ 10^{-18} esu). With α of 4–10 Å³, μ is only about one tenth of αF_c. Here, as in all other investigations,[12,13] μ is omitted from the equation. Our data for α may therefore be ~10% too high.

The experimental conditions and the velocities of the directional walk for 5-d transition-metal adatoms on the W (110) planes obtained are given in

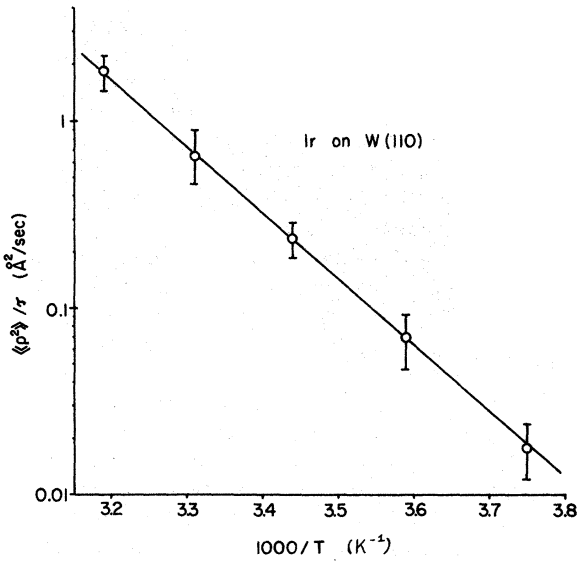

FIG. 5. Temperature dependence of the random-walk diffusion (no driving force) of a single Ir adatom on a W (110) plane. From the plot, we find $E_d = 0.70$ eV and $D_0 = 1\times10^{-5}$ cm²/sec.

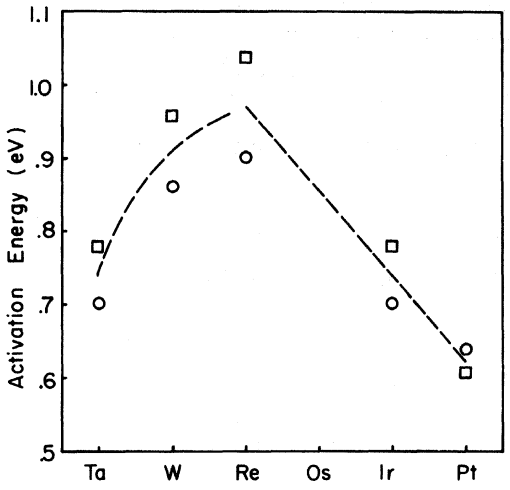

FIG. 6. Activation energy of the 5-*d* transition-metal adatoms on the W (110) plane. □ are data points from Ref. 3. ○ are data points from this investigation. In contrast to Ref. 3 where data were obtained from a few adatoms on a plane, all of our data points were derived from a single adatom on a perfect plane.

Table I. The adatom polarizabilities as derived from Eq. (27) are also listed in the table. It is most interesting to note that the polarizability of adatoms decreases in the order of Ta, W, Re, Ir, and Pt. This *d*-electron dependence is therefore quite different from that for the activation energy of surface migration. While theoretical values for the adatom polarizability α are unavailable, values for the polarizability of free atoms α_a from self-consistent-field calculations do exist.[25] These values are also listed in Table I. It is interesting to note that both α and α_a decrease monotonically from Ta to Pt. The ratio α/α_a, as shown in Fig. 7, however, changes from 0.66 for Ta adatom to 0.24 for Pt adatom. This wide range of the ratio indicates that a chemical specific charge-transfer effect takes place between the adatoms and the substrate surface. Such a charge-transfer effect is expected from the present theory of chemisorption, as will be discussed in Sec. IV.

The gas-pressure dependence of the directional walk was investigated with Ir adatoms at two image-gas pressures. The reason for choosing Ir was that if the image gas does affect the accuracy of the experiment, it would show up with Ir most clearly, because of all the adatoms investigated, the directional-walk field for Ir is one of the highest. At 2×10^{-4} Torr helium, the polarizability obtained is 3.28 ± 0.38 Å^3. By reducing the gas pressure by a factor of 3, a value of 3.74 ± 0.33 Å^3 is obtained. These two values are within the statistical errors specified. The fact that Ir and Pt, which are measured under the highest applied fields, have the smallest polarizabilities, also indicates that the electron shower does not play a significant role.

It is also important to note that for the physical conditions indicated, the adatoms moved almost exclusively in the direction of maximum field gradient, i.e., in the radial direction of the plane. This can be seen in both Figs. 3 and 4. The temperature where the directional walk becomes detectable is nearly the same as that for the random walk. We therefore conclude that on a smooth plane such as the W (110), the effect of ΔF, $\Delta\mu$, and $\Delta\alpha$, as defined in Eq. (10), is small. As $\Delta\alpha$ even on the rough W(111) plane[13] is only ~20% of the adatom polarizability that we obtained, it is estimated that the error introduced by omitting these secondary effects is perhaps less than 5%.

C. Polarizability of adatoms

The polarizabilities of free atoms and molecules have long been a subject of considerable interest to theoretical as well as experimental investigations. It is well known that the van der Waals-London force can be expressed as a function of the polarizabilities of the two interacting atoms. Comprehensive reviews of the subject exist.[26–28]

The polarizability of an adatom is different from the free-atom polarizability due to at least two effects, namely, the screening by surface charges and the charge transfer between the adatom and the substrate plane. The former effect has been long realized and has been discussed in some detail earlier.[17] It was found that the polarizability of a

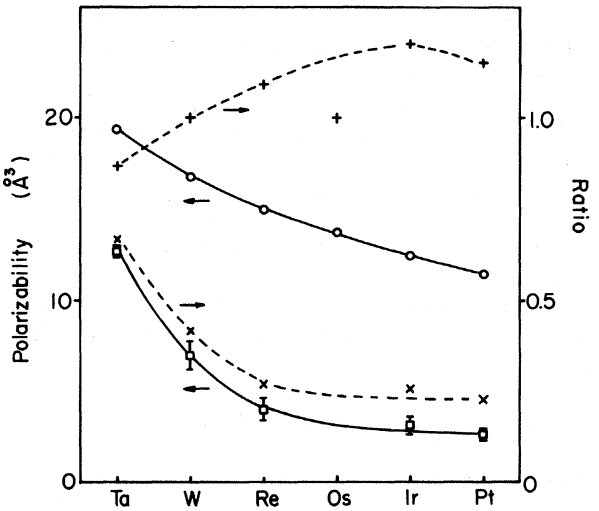

FIG. 7. Adatom polarizabilities α are represented by □, the free-atom polarizabilities α_a obtained by Thorhallson *et al.* are represented by ○. × represents the rations α/α_a. The +'s are the ratios of the desorption field of an adatom with that of a W adatom, as obtained by Plummer and Rhodin. The fact that α/α_a varies from 0.66 for Ta to 0.24 for Pt indicates the occurrence of a chemical specific charge transfer between the adatoms and the substrate surface.

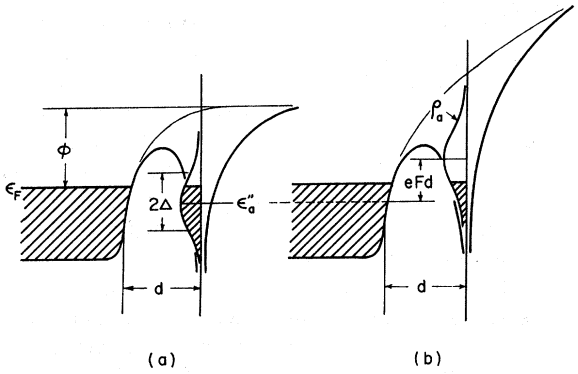

FIG. 8. (a) Generally accepted view of chemisorption. An adatomic level is broadened into a band of width 2Δ. ϵ_a'' denotes the center of the band. (b) When a positive electric field F is applied, the center of the band shifts upward by an amount eFd. As a result, the electronic charge localized near the adatom is greatly reduced. This field-dependent charge-transfer effect is responsible for the polarizability of the chemisorbed atom.

physisorbed atom depends on the atom-to-surface mirror plane distance.[17] Here we point out without elaboration how a chemisorbed adatom's polarizability may depend on the electronic density of states of the adatom.

It is generally accepted that the energy levels of a chemisorbed atom are both shifted and broadened into bands,[29-31] as shown schematically in Fig. 8(a). A charge transfer between the adatom and the surface is responsible for the surface-induced dipole moment of the adatom.[32] As shown in Fig. 8(b), when an electric field F is applied, the broadened energy levels will be shifted upward by an amount eFd, where d is the adatom-to-surface plane distance. As a result, the surface dipole moment will be changed by an amount $\Delta\mu_F$. By the definition of the polarizability, we have

$$\Delta\mu_F \equiv \alpha F$$
$$= (-e)d\int_{-\infty}^{\epsilon_F - eFd} \rho_a(\epsilon)d\epsilon - (-e)d\int_{-\infty}^{\epsilon_F} \rho_a(\epsilon)d\epsilon\,, \tag{28}$$

$$\alpha = \frac{ed}{F}\int_{\epsilon_F - eFd}^{\epsilon_F} \rho_a(\epsilon)d\epsilon\,, \tag{29}$$

where $\rho_a(\epsilon)$ is the total density of states of the adatom and ϵ_F is the Fermi level. In general, the adatom density of states are Lorentzian.[29] Thus

$$\alpha = \frac{ed}{\pi F}\sum_i \left(\tan^{-1}\frac{\epsilon_F - \epsilon_{ai}''}{\Delta_i} - \tan^{-1}\frac{\epsilon_F - \epsilon_{ai}'' - eFd}{\Delta_i}\right), \tag{30}$$

where Δ_i is the width and ϵ_{ai}'' is the center of the ith adatomic orbital. This equation is similar to that given by Gadzuk for the surface dipole moment of an adatom.[32] However, the adatom polarizability is a more straightforward quantity and shows a simpler form. For comparison with our data, Eq. (29) is written in the form

$$\alpha = e^2 d^2 \bar{\rho}_a\,, \tag{31}$$

where $\bar{\rho}_a$ is the average density of states in the energy range between $\epsilon_F - eFd$ and ϵ_F. Although, in principle, one should be able to derive the density of states $\rho_a(\epsilon)$ as a function of ϵ from Eq. (29), in this first report, only the average density of states $\bar{\rho}_a$ will be estimated from Eq. (31). Accurate values for the adatom-to-surface plane distance d are unavailable, but they should be about 1 Å. Since the atomic radius of all the adatoms should be nearly equal, the d-electron dependence of the adatom polarizability (Fig. 7) should also reflect that of the average total density of states near the Fermi level. For W adatoms on the W (110) plane, the distance d has been estimated to be ~0.8 Å from an investigation of the field-evaporation rate.[15] Using this value, the absolute value of the average total density of states is found to be $\bar{\rho}_a \approx 0.75$ eV^{-1} for an adatom, which is physically a very reasonable value. We recognize here, of course, that a further elaborate investigations are needed to obtain accurate data on the adatom density of states. But it is now clear that a close connection between the adatom polarizability and the adatom density of states exists.

The adatom polarizability is also an important parameter in the theory of field desorption.[14,20] For an adatom with a polarizability of a few Å^3 at a field of 4–5 V/Å, the polarization binding energy amounts to 3–5 eV, which is comparable to the binding energy of the adatom with the substrate plane. Although the adatom binding energies can be rederived by including the polarization binding, information on the charge state of the adatoms in the field desorption process is not yet available. Since the adatom polarizability decreases monotonically from Ta to Pt, the inclusion of the polarization bindings probably will not alter the *qualitative* feature of the adatom binding energy of 5-d transition metal adatoms on the tungsten surface.[16] This conclusion is supported by the similar d-electron dependence of the activation energy of surface diffusion of the same adatoms. The rederivation of the binding energies has to await the determination of charge states of the field-desorbed ions.

V. SUMMARY

The directional walk of 5-d transition-metal adatoms on the W (110) plane under a driving force has been investigated in the field-ion microscope. The driving force arises from a polarization binding in a nonuniform electric field. The electric field needed to produce an observable directional walk ranges from ~1.9 V/Å for Ta adatoms to

~4.5 V/Å for Pt adatoms. From the velocity of the directional walk, the adatom polarizabilities of 5-*d* transition-metal adatoms have been derived. The adatom polarizability decreases monotonically from Ta adatoms to Pt adatoms. The advantages of deriving the adatom polarizability from the directional walk are: (a) The method gives the true polarizability, not the difference in the polarizability of the adatom between two different sites. (b) The crystal planes are well defined to an atomic level. (c) Since all the measurements were done with a single adatom, no interaction with other adatoms occurred.

The polarizability of a chemisorbed atom is very different from that of a free atom. While the polarizability of a free atom arises from a field induced deformation of the electronic charge distribution, the polarizability of a chemisorbed metallic atom arises mostly from a field-induced charge transfer between the adatom and the substrate surface and partly from a screening effect by the surface charges. Although there is still no comprehensive theory dealing with the adatom polarizability, using the present view of chemisorption, it is obvious that the adatom polarizability is closely connected to the adatom density of states. We estimate the average density of states of a W adatom on the W (110) plane, in the -5.3 to -7.2 eV range, to be about 0.75 eV^{-1}, where 5.3 eV is the work function of the plane and 7.2 eV $= \phi + eFd$. Clearly, for a more meaningful analysis, a better quantitative theory of chemisorption has to be developed.

Although the polarization bindings at the desorption fields of the adatoms are considerable, since the adatom polarizability decreases monotonically from Ta to Pt adatoms, they probably will not alter the *qualitative* validity of the binding-energy measurements. The quantitative data of the adatom binding energy can be derived by including the polarization binding when the charge state of the adatoms in the field desorption process are established. Such information is not yet available.

The interaction between two chemisorbed adatoms arises mainly from an indirect interaction as has been discussed by Grimley[33]; and Einstein and Schrieffer.[34] The interaction depends on the density of states of the adatoms; thus, it is directly related to the adatom polarizability. While a theoretical treatment of such a relation is not available, an experimental measurement of the cohesive energy of diatomic clusters on the W (110) plane by Bassett and Tice[35] shows that $E_{\mathrm{Ta\text{-}Ta}} > E_{\mathrm{W\text{-}W}} > E_{\mathrm{Re\text{-}Re}}$. This result is consistent with that expected from our adatom polarizability data.

Note added in proof. We have been informed that a qualitative discussion of the field-induced surface diffusion was first given by Drechsler in connection with a field-emission-microscope investigation.[35]

ACKNOWLEDGMENTS

The authors appreciate very much the continued interest of Professor E. W. Müller, and the technical assistance of Paul Cowan, G. L. Fowler, and S. B. McLane.

*Supported by the National Science Foundation.
[1]E. W. Müller, Z. Elektrochem. 61, 43 (1957).
[2]G. Ehrlich and F. G. Hudda, J. Chem. Phys. 44, 1039 (1966).
[3]D. W. Bassett and M. J. Parsley, Br. J. Appl. Phys. 2, 13 (1969).
[4]T. T. Tsong, Phys. Rev. B 6, 417 (1972).
[5]G. Ayrault and G. Ehrlich, J. Chem. Phys. 60, 281 (1974).
[6]T. T. Tsong and R. J. Walko, Phys. Status Solidi A 12, 111 (1972).
[7]G. Ehrlich, J. Chem. Phys. 44, 1050 (1966).
[8]T. T. Tsong, P. Cowan, and G. Kellogg, Thin Solid Films 25, 97 (1975).
[9]T. T. Tsong, Phys. Rev. B 7, 4018 (1973).
[10]P. Bettler and F. M. Charbonnier, Phys. Rev. 119, 85 (1960).
[11]H. Utsugi and R. Gomer, J. Chem. Phys. 37, 1706 (1962).
[12]L. W. Swanson, R. W. Strayer, and F. M. Charbonnier, Surf. Sci. 2, 177 (1964).
[13]W. R. Graham and G. Ehrlich, Surf. Sci. 45, 530 (1974).
[14]R. Gomer and L. W. Swanson, J. Chem. Phys. 38, 1613 (1963).
[15]T. T. Tsong, J. Chem. Phys. 54, 4205 (1971).
[16]E. W. Plummer and T. N. Rhodin, J. Chem. Phys. 49, 3499 (1968).
[17]T. T. Tsong and E. W. Müller, J. Chem. Phys. 55, 2884 (1971).
[18]R. D. Young, in *7th Field Emission Symposium* (McMinnville, Oregon, 1960); G. Ehrlich and F. G. Hudda, Philos. Mag. 8, 1587 (1963).
[19]See, for example, F. O. Goodman, in *Progress in Surface Science*, edited by S. G. Davidson (Pergamon, New York, 1974), Vol. 5, Pt. 3.
[20]C. A. Bennett (private communication). See also the abstracts of the Int. Conf. on Low Temp. Diffusion and Apy. to Thin Films, August, 1974 (Elsevier, Lausanne, 1975).
[21]See, for example, E. W. Müller and T. T. Tsong, *Field Ion Microscopy, Principles and Applications* (American Elsevier, New York, 1969); Prog. Surf. Sci. 4, 1 (1974), edited by S. G. Davison.
[22]T. Sakurai and E. W. Müller, Phys. Rev. Lett. 30, 532 (1973).
[23]E. W. Plummer and T. N. Rhodin, Appl. Phys. Lett. 11, 194 (1967).
[24]K. Besocke and H. Wagner, Phys. Rev. B 8, 4597 (1973).
[25]J. Thorhallsson, C. Fisk, and S. Fraga, J. Chem. Phys. 49, 1987 (1968).
[26]H. Margenau, Rev. Mod. Phys. 11, 1 (1939).

[27]A. Dalgarno, Adv. Phys. 11, 281 (1962).
[28]A. D. Buckingham and B. J. Orr, Q. Rev. Lond. 21, 195 (1967).
[29]A. J. Bennett and L. M. Falicov, Phys. Rev. 151, 512 (1966).
[30]J. W. Gadzuk, Surf. Sci. 6, 133 (1967).
[31]R. Gomer, CRC Critical Rev. Solids State Sci. 4, 247 (1974).
[32]J. W. Gadzuk, in *The Structure and Chemistry of Solid Surfaces*, edited by G. A. Somorjai (Wiley, New York, 1969), p. 43–13.
[33]T. B. Grimley, Proc. Phys. Soc. Lond. 90, 751 (1967); 92, 776 (1967).
[34]T. L. Einstein and J. R. Schrieffer, Phys. Rev. B 7, 3629 (1973).
[35]D. W. Bassett and D. R. Tice, 21st Field Emission Symposium (Marseille, France, July 1974).
[36]M. Drechsler, Z. Elektrochem. 61, 48 (1957).

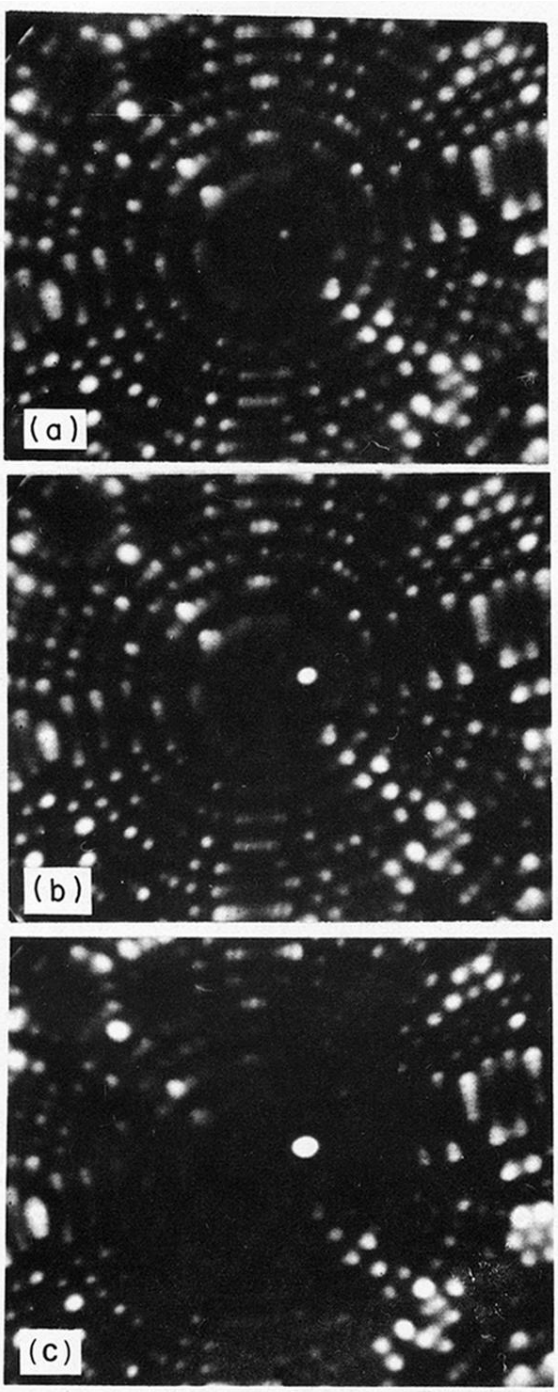

FIG. 3. Helium FI micrographs showing the directional walk of an Ir adatom on a W (110) plane. Between two sucessive adatom locations, the emitter was maintained at 296 °K with an applied field of 3.9 V/Å for 15 sec. The micrographs were taken at 4.5 V/Å and 78 °K.

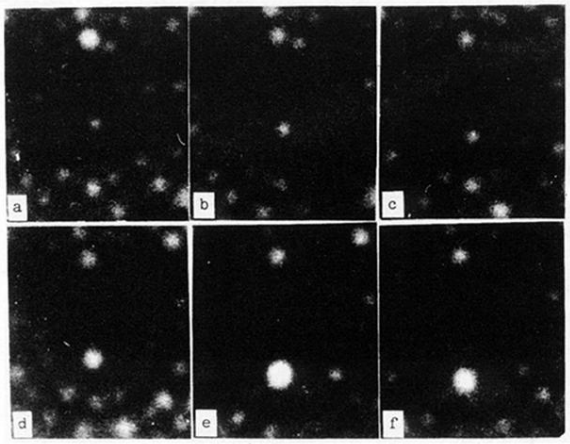

FIG. 4. Continuous observation of the directional walk of a W adatom on a W (110) plane at ~3.8 V/Å and ~295 °K. A Ne-Ar mixed gas of $\sim 6\times10^{-3}$ Torr was used for the imaging. The good contrast of the image at such a high temperature results from the field adsorption of Ar atoms. Although the directional walk of the adatom was most vividly seen with this technique, it was not used to derive the quantitative data. The reasons are discussed in the text.